

Kinetics and Mechanism of the Copper-Catalysed Oxygenation of 2-Nitropropane

Éva Balogh-Hergovich,^[a] Zoltán Grécsi,^[b] József Kaizer,^[a] Gábor Speier,^{*,[a]}
Marius Réglier,^[c] Michel Giorgi,^[c] and László Párkányi^[d]

Keywords: 2-Nitropropane / Copper nitronates / Oxygenation / Copper / Kinetics / Dioxygenase

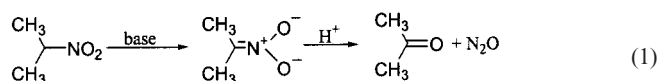
Primary and secondary nitro compounds react with dioxygen in the presence of copper metal and N ligands such as *N,N,N',N'*-tetramethylethylenediamine (tmeda), 2,2'-bipyridine (bpy), and 1,10-phenantroline (phen) in various solvents to form aldehydes or ketones. More coordinating solvents as well as donor N ligands accelerate the reaction remarkably. The oxygenolysis of 2-nitropropane (NPH) in the presence of copper and tmeda in DMF results in acetone and acetone oxime. The amount of tmeda influences the chemoselectivity, higher tmeda concentrations preferentially lead to the formation of the oxime. The kinetics of the reaction, measured at 90 °C, resulted in a rate equation of first-order dependence on copper and dioxygen and second-order dependence on 2-nitropropane. The rate constant, activation

enthalpy, and entropy at 363.16 K are as follows: $k_{\text{cat}} = (5.37 \pm 0.34) \times 10^{-2} \text{ mol}^{-3} \text{ dm}^9 \text{ s}^{-1}$, $E_a = 131 \pm 4 \text{ kJ mol}^{-1}$, $\Delta H^\ddagger = 127 \pm 4 \text{ kJ mol}^{-1}$ and $\Delta S^\ddagger = 80 \pm 13 \text{ J mol}^{-1} \text{ K}^{-1}$. The catalytically active intermediates $\text{Cu}^{\text{II}}(\text{NP})_2(\text{tmeda})$ and $\text{Cu}^{\text{II}}(\text{NO}_2)_2(\text{tmeda})$ in the catalytic cycle were isolated and their structures determined by X-ray crystallography. The kinetics of the stoichiometric oxygenation of $\text{Cu}^{\text{II}}(\text{NP})_2(\text{tmeda})$ to $\text{Cu}^{\text{II}}(\text{NO}_2)_2(\text{tmeda})$ and acetone resulted in the overall second-order rate equation with a rate constant, activation enthalpy, and entropy at 313.16 K of $k_s = 0.46 \pm 0.02 \text{ mol}^{-1} \text{ dm}^3 \text{ s}^{-1}$, $E_a = 38 \pm 1 \text{ kJ mol}^{-1}$, $\Delta H^\ddagger = 35 \pm 1 \text{ kJ mol}^{-1}$ and $\Delta S^\ddagger = -142 \pm 13 \text{ J mol}^{-1} \text{ K}^{-1}$, respectively.

© Wiley-VCH Verlag GmbH, 69451 Weinheim, Germany, 2002

Introduction

The transformation of primary and secondary aliphatic nitro compounds to aldehydes or ketones is a reaction often used in organic chemistry and in biological processes as well. The Nef reaction, the classical method for this conversion, involves the hydrolysis of the conjugate bases of nitroalkanes with sulfuric acid [Equation (1)].^[1]



There are also a fair number of stoichiometric reagents for this conversion. Treatment of nitroalkanes with aqueous TiCl_3 ,^[2] cetyltrimethylammonium permanganate,^[3] tin complexes and NaHSO_3 ,^[4] activated dry silica gel,^[5] 30% $\text{H}_2\text{O}_2/\text{K}_2\text{CO}_3$,^[6] KMnO_4 ,^[7] ceric ammonium nitrate (CAN),^[8] $\text{MoO}_5/\text{pyridine}/\text{HMPA}$,^[9] ozone^[10] or singlet oxygen^[11] leads to oxo compounds; *t*BuOOH and a catalyst provide a catalytic process for the transformation.^[12]

Biochemical degradation of aliphatic nitro compounds is also known in the literature. Glucose oxidase and D- and L-amino acid oxidase accept nitroalkane anions as substrates.^[13] The flavoenzyme-catalysed oxidation of nitroalkanes and its mechanism has been established.^[14,15] Electron-deficient flavins also oxidise nitroalkane anions in model reactions.^[16,17]

Extracts of *Neurospora crassa* and pea seedlings oxidatively metabolise nitroethane and nitropropane,^[18] and those from the hyphae of a nitrifying strain of *Aspergillus flavus* produce nitrite and nitrate from 2-nitropropane.^[19] 2-Nitropropane and some other nitroalkanes are oxidatively denitrified by an intracellular enzyme of *Hansenula mraki*.^[20] 2-Nitropropane dioxygenase has been purified and characterised as an iron-containing metalloenzyme.^[21] It belongs to the peculiar class of intermolecular dioxygenases catalysing the reaction according to Equation (2).^[22] That means

^[a] Research Group for Petrochemistry, Hungarian Academy of Sciences, 8201 Veszprém, Hungary

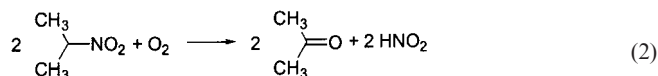
^[b] Department of Organic Chemistry, University of Veszprém, 8201 Veszprém, Hungary
Fax: (internat.) + 36-88/427-492
E-mail: speier@almos.vein.hu

^[c] Université d'Aix-Marseille 1 et 3, Faculté des Sciences et Techniques de Saint-Jérôme, Chimie, Biologie et Radicaux Libres, UMR CNRS, 6517, Case 432, Avenue Escadrille Normandie-Niemen, 13397 Marseille Cedex 13, France

^[d] Chemical Research Center, Hungarian Academy of Sciences, 1525 Budapest, Hungary

Supporting information for this article is available on the WWW under <http://www.eurjic.com> or from the author.

that the two oxygen atoms of dioxygen are incorporated into two molecules of the substrate.



In order to gain more insight into the mechanism of these reactions we initiated studies on copper- and iron-mediated oxygenations of nitroalkanes. We could show that isopropyl nitronate, ligated to a copper ion, can be oxygenated to (nitrito)copper species and acetone,^[23] and in the presence of copper metal, as a precursor, nitroalkanes are easily transformed to aldehydes or ketones by dioxygen.^[24] In this paper we present kinetic and spectroscopic data on this reaction, the X-ray structures of intermediates and propose a plausible mechanism for the oxygenation as a 2-nitropropane dioxygenase mimicking reaction.

Results and Discussion

Stoichiometric Oxygenation

To a 2-nitropropane (NPH) solution in DMF, copper metal powder was added under dioxygen. The colour of the solution slowly turned reddish and further dissolution of the solid copper resulted in a green homogeneous solution. If coordinating N ligands, such as *N,N,N',N'*-tetramethylethylenediamine (tmeda), 2,2'-bipyridine (bpy), or 1,10-phenanthroline (phen) were also present, the dissolution of the copper metal proceeded even faster. According to parallel gas-volumetric (O_2), titrimetric (NO_3), spectrophotometric (NO_2) and GC (acetone) measurements (Table 1), the stoichiometry of the oxygenation reaction corresponds to Equation (3). Figure 1 shows typical dioxygen uptake vs. time curves for the oxidation process obtained by the gas-volumetric method.

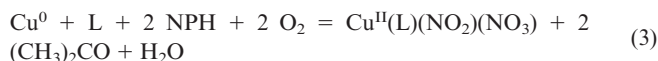


Table 1. Stoichiometric oxygenation of 2-nitropropane in DMF solution in the absence and presence of N ligands

Expt. no.	Ligand	Conv. ^[a] %	NO_3 ^[b] mmol	NO_2 ^[c] mmol	Conv. ^[d] %	Conv. ^[e] %
1	—	12	0.22	0.09	9.3	10
2	tmeda	98	0.98	1.20	73	87
3	phen	91	0.89	1.01	63	78
4	bpy	73	0.99	1.06	68	72

^[a] Conversions were determined by gas volumetry. ^[b] Yields were determined by titrimetry. ^[c] Yields were determined by spectrophotometry. ^[d] Conversions were determined from ^[b] and ^[c]. ^[e] Conversions were determined by GLC.

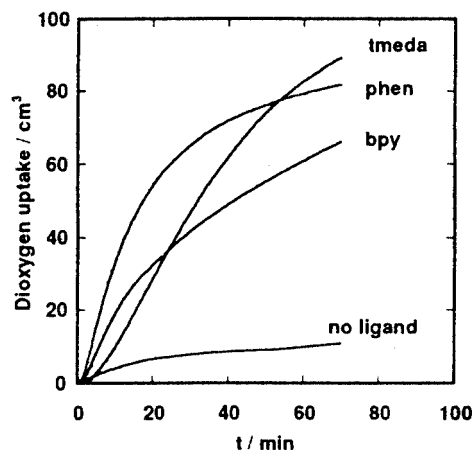
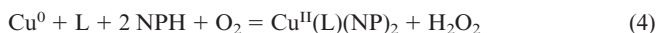


Figure 1. Time course for the stoichiometric oxygenation of 2-nitropropane in the presence of copper metal and N-containing ligands (bpy, phen, tmeda); $\text{Cu}^0 = \text{L} = 1.5 \text{ mmol}$, $\text{NPH} = 3 \text{ mmol}$, 90°C , 30 mL DMF

The presence of the intermediate H_2O_2 in the reaction mixture could be demonstrated either by iodometry or oxidising triphenylphosphane to triphenylphosphane oxide. We believe that in the first step copper metal, in the presence of N ligands, reacts with the *aci* form of the secondary nitro compound to give copper nitronate complexes and H_2O_2 [Equation (4)]. Similar reactions were reported for the reaction of copper metal with acidic compounds in the presence of air.^[25]



In the presence of molecular oxygen both copper(I) and copper(II) nitronates are probably first formed, the former is then transformed to $\text{Cu}^{\text{II}}(\text{L})(\text{NP})_2$, which can be oxygenated to the desired products [Equation (5)].



This is then followed by the fast consecutive formation of $\text{Cu}^{\text{II}}(\text{L})(\text{NO}_2)(\text{NO}_3)$, which is assumed to be obtained as a product of the oxidative process between $\text{Cu}^{\text{II}}(\text{L})(\text{NO}_2)_2$ and H_2O_2 [Equation (6)].



Copper-Catalysed Oxygenation of 2-Nitropropane

Previously we have reported that primary and secondary nitro compounds in the presence of copper metal and N ligands can be transformed to aldehydes or ketones and HNO_2 . The reaction can also be carried out catalytically in

the presence of tmeda at high 2-nitropropane/copper ratios in a very efficient way (Figure 2).

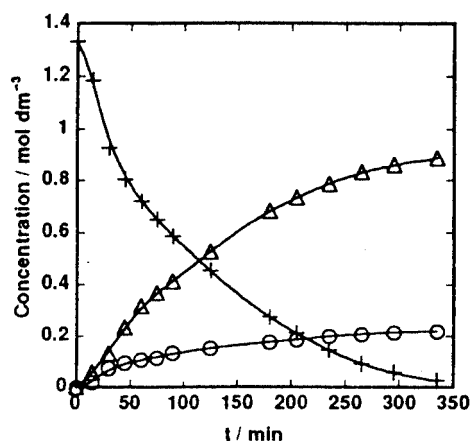
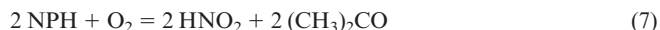


Figure 2. Time course for the copper-catalysed oxygenation of 2-nitropropane (+) [acetone (Δ); acetone oxime (o)] in DMF using tmeda as ligand (Experiment 3, Table 4)

In these experiments Cu^0 , tmeda, and 2-nitropropane are first pretreated with O_2 to give a homogeneous solution in about 10–15 min and thereafter the reaction takes place in a homogeneous phase. According to simultaneous gas-volumetric and GC measurements the stoichiometry of the oxidation reaction corresponds to that shown in Equation (7).



In the reaction mixture the presence of acetone oxime is also detected (10–20%). The formation of acetone oxime is favoured at high tmeda concentrations (Figure 3). We believe that excess tmeda acts as a base and in the presence of HNO_2 the salt $\text{tmeda} \cdot \text{HNO}_2$ is formed, which reacts with 2-nitropropane resulting in the oxime [Equation (8)].

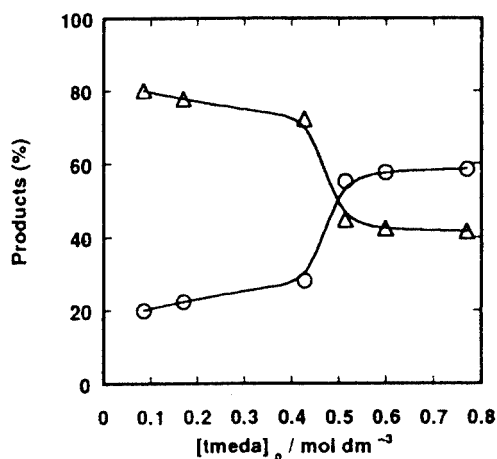
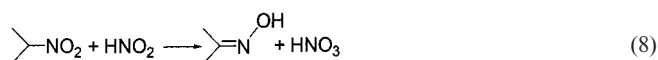


Figure 3. Plots of amounts of acetone (Δ) and acetone oxime (o) formed vs. the initial tmeda concentration at the copper-catalysed oxygenation of 2-nitropropane in DMF (Experiment 15, Table 4)



On addition of ether to the reaction mixture, a green solid precipitated from which, after recrystallisation from ethanol, green crystals of $\text{Cu}^{\text{II}}(\text{NO}_2)_2(\text{tmeda})$ were obtained. The presence of $\text{Cu}^{\text{II}}(\text{NO}_2)_2(\text{tmeda})$ in the reaction mixture clearly suggests that the first step in the catalytic oxygenation of 2-nitropropane is the formation of the fairly stable $\text{Cu}^{\text{II}}(\text{NP})_2(\text{tmeda})$ complex from copper powder, 2-nitropropane, tmeda and dioxygen, which further rapidly reacts with dioxygen to form the more stable nitrito species $\text{Cu}^{\text{II}}(\text{NO}_2)_2(\text{tmeda})$. The complex $\text{Cu}^{\text{II}}(\text{NP})_2(\text{tmeda})$ was prepared by the stoichiometric reaction of $\text{Cu}^{\text{II}}(\text{OMe})_2$, 2-nitropropane and tmeda in THF under Ar.

Characterisation of $\text{Cu}^{\text{II}}(\text{NO}_2)_2(\text{tmeda})$

$\text{Cu}^{\text{II}}(\text{NO}_2)_2(\text{tmeda})$ displays three bands at 1360, 1286 and 808 cm^{-1} in its IR spectrum assigned to the asymmetric and symmetric stretching and bending frequencies of the nitro group. There are three additional bands at 953, 845 and 593 cm^{-1} due to deformation and bending frequencies of the nitro group. Three bands at 2983, 2941 and 2899 cm^{-1} can be assigned to the ligand tmeda coordinated to the copper ion. The electronic absorption spectrum of $\text{Cu}^{\text{II}}(\text{NO}_2)_2(\text{tmeda})$ in acetonitrile showed two intense bands at 271 and 222 nm, which were assigned to LMCT bands. Further, the LMCT bands for the nitro complex at 271 nm may include contributions from the $n \rightarrow \pi^*$ transition as well.^[26] Crystallographic characterisation of $\text{Cu}^{\text{II}}(\text{NO}_2)_2(\text{tmeda})$ shows that the molecule is monomeric. The view of the molecule depicted in Figure 4 shows that the copper(II) centre has an elongated rhombic octahedral geometry with a $\text{CuO}_2\text{N}_2\text{O}_2$ chromophore and a $(4+2^*)$ -type coordination involving two off-the- z -axis bonds.

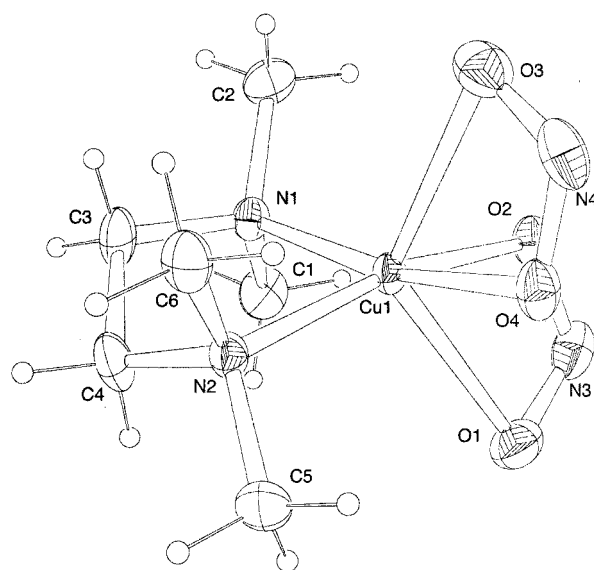


Figure 4. Molecular structure and numbering scheme of $[\text{Cu}^{\text{II}}(\text{NO}_2)_2(\text{tmeda})]$ (1); only one molecule is shown; hydrogen atoms are omitted for clarity, the ellipsoids represent a probability of 40%

Selected bond lengths and angles given in Table 2 show that two N atoms of the bidentate *N,N,N',N'*-tetramethylethylenediamine ligand with Cu–N distances of 2.0291(4) and 2.0242(4) Å, and two O atoms of the NO₂ ligands with Cu–O distances of 2.0052(4) and 2.0087(4) Å, occupy basal positions, the other two O atoms of the NO₂ ligands with Cu–O distances of 2.3992(5) and 2.4693(5) Å being in apical positions. This is associated with the bidentate bonding mode of oxyanions to the copper(II) ion, such as the nitrite and nitrate anions, all of which form good primary ligands to the copper(II) ion as in [Cu^{II}(pyrazine)₂(O₂NO₂)₂]^[27] and [Cu^{II}(bipy)(ONO)₂]^[28]. Asymmetric bidentate copper nitrite coordination was also found in other complexes with N-donor ligands.^[29,30]

Table 2. Selected bond lengths [Å] and angles [°] for [Cu^{II}(NO₂)₂(tmeda)]

Cu1–O2	2.0052(4)
Cu1–O3	2.3992(5)
Cu1–O4	2.0087(4)
Cu1–N1	2.0291(4)
Cu1–N2	2.0242(4)
Cu1–O1	2.4693(5)
O1–O2	2.0898(7)
O1–N3	1.2380(7)
O2–N3	1.2700(7)
O3–O4	2.0972(6)
O3–N4	1.2279(7)
O4–N4	1.2784(7)
N1–C1	1.4805(7)
N1–C2	1.4815(8)
N1–C3	1.4851(7)
N2–C4	1.4794(7)
N2–C5	1.4830(7)
N2–C6	1.4766(7)
C3–C4	1.4838(9)
C5–C6	2.3891(10)
O2–Cu1–O3	86.99(2)
O2–Cu1–O4	89.602(15)
O2–Cu1–N1	93.13(2)
O2–Cu1–N2	166.78(2)
O3–Cu1–O4	55.98(2)
O3–Cu1–N1	111.63(2)
O3–Cu1–N2	105.41(2)
O4–Cu1–N1	167.18(2)
O4–Cu1–N2	93.57(2)
O1–Cu1–O2	54.49(2)
O1–Cu1–N1	106.08(2)
O1–Cu1–N2	112.92(2)
N1–Cu1–N2	86.61(2)
O2–O1–N3	34.06(3)
Cu1–O2–O1	74.14(2)
Cu1–O2–N3	107.18(4)
O1–O2–N3	33.09(3)
Cu1–O3–O4	52.547(15)
Cu1–O3–N4	86.48(4)
O4–O3–N4	33.96(3)
Cu1–O4–O3	71.47(2)
Cu1–O4–N4	103.89(3)
O3–O4–N4	32.45(3)
Cu1–N1–C1	111.97(3)
Cu1–N1–C2	109.26(3)
Cu1–N1–C3	106.23(3)

Characterisation of Cu^{II}(NP)₂(tmeda)

The green complex Cu^{II}(NP)₂(tmeda) was prepared in 85% yield. The IR spectrum of the complex shows intense sharp bands corresponding to the coordinated *aci*-2-nitropropanate ligands at 1612 [ν (C=N)], 1162 and 1123 [$\nu_{\text{as}}(\text{NO}_2)$], and 943 [$\nu_{\text{s}}(\text{NO}_2)$] cm^{−1}. The electronic spectrum of the complex shows an absorption band at 727 nm due to d-d transitions. A higher energy band at 314 nm is associated with charge transfer transition. Room-temperature magnetic measurements yielded a value of $\mu_{\text{eff}} = 1.92$ BM for the complex consistent with a copper(II) ion. The view of the molecule in Figure 5 shows that the geometry around the copper(II) centre is similar to that of the Cu^{II}-(NO₂)(tmeda) complex with an elongated rhombic octahedral CuO₂N₂O₂ chromophore and a (4+2*)-type coordination, involving two off-the-z-axis bonds. Selected bond lengths and angles given in Table 3 show that two N atoms of the bidentate *N,N,N',N'*-tetramethylethylenediamine ligand, with Cu–N distances of 2.0665(14) Å, and two O atoms of the nitronate ligands, with Cu–O distances of 1.9997(13) Å, occupy basal positions, while the other two O atoms of the nitronate ligands, with Cu–O distances of 2.3615(13) Å, are in apical positions. The carbon–nitrogen bond [1.290(2) Å] in the nitronate ligand is essentially double bond in character (C–N 1.47 Å, C=N 1.27 Å).^[31] This is similar to the findings for the structures of Cu^I(NP)(PPh₃)₂^[23] and Fe^{III}(NP)₃.^[32] The C–N distances are somewhat longer in Cu^{II}(NP)₂ (1.34–1.35 Å), however, its structure consists of chains of Cu^{II}(NP)₂ units.^[33]

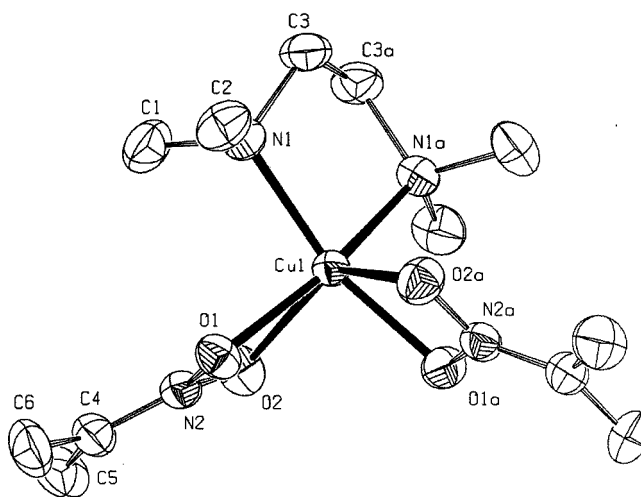


Figure 5. Molecular structure and numbering scheme of [Cu^{II}-(NP)₂(tmeda)] (2); only one molecule is shown; hydrogen atoms are omitted for clarity, the ellipsoids represent a probability of 40%

Kinetic Measurements

The reaction between 2-nitropropane and dioxygen in the presence of a catalytic amount of copper and tmeda were performed in DMF solution and examined in the temperature range 363.16 to 373.16 K with a ratio between initial concentrations of copper and 2-nitropropane in the range

Table 3. Selected bond lengths [Å] and angles [°] for [Cu^{II}-(NP₂)₂(tmeda)]

Cu1–O1	1.9997(13)
Cu1–N1	2.0665(14)
Cu1–O2	2.3615(13)
O1–N2	1.3360(18)
O2–N2	1.3205(19)
N1–C1	1.472(2)
N1–C2	1.479(2)
N1–C3	1.481(2)
N2–C4	1.290(2)
C3–C3	1.508(4)
C4–C6	1.477(3)
C4–C5	1.497(3)
O1–Cu1–O1	98.86(7)
O1–Cu1–N1	90.64(6)
O1–Cu1–N1	161.00(5)
O1–Cu1–N1	161.00(5)
O1–Cu1–N1	90.64(6)
N1–Cu1–N1	85.30(8)
O1–Cu1–O2	93.19(5)
O1–Cu1–O2	60.51(5)
N1–Cu1–O2	102.79(5)
N1–Cu1–O2	105.80(5)
O1–Cu1–O2	60.51(5)
O1–Cu1–O2	93.20(5)
N1–Cu1–O2	105.80(5)
N1–Cu1–O2	102.79(5)
O2–Cu1–O2	140.79(7)
N2–O1–Cu1	100.13(10)
N2–O2–Cu1	84.51(9)

1:6–33. Experiments were also carried out at different dioxygen concentrations. Experimental conditions are summarised in Table 4.

A simple rate law for the catalytic reaction between 2-nitropropane and dioxygen catalysed by copper in the presence of tmeda is given in Equation (9).

$$-d[\text{NPH}]/dt = d[\text{acetone}]/dt = k_{\text{cat}}[\text{NPH}]^m[\text{Cu}]^n[\text{O}_2]^q \quad (9)$$

In order to determine the rate dependence on the various reactants, oxygenation runs were performed at different substrate concentrations (Table 4; Experiments 1–4), catalyst concentrations (Table 4; Experiments 3, 5–9), and at different dioxygen pressures (Table 4; Experiments 10–14). Assuming a constant concentration of the catalyst during each reaction, as well as a constant dioxygen pressure for the experiments, the pseudo-first-order rate law according to Equation (10) is obtained, where $k_{\text{cat}}' = k_{\text{cat}}[\text{Cu}]^n[\text{O}_2]^q$.

$$-d[\text{NPH}]/dt = k_{\text{cat}}'[\text{NPH}]^m \quad (10)$$

Plots of $[\text{NPH}]^{-1}$ vs. time were linear in Experiments 1–14, indicating that the reaction is second order with respect to substrate concentration. Columns k_{cat}' and R in Table 4 report slopes and the correlation coefficients obtained by the least-squares method for these linear regressions. From variations of the reaction rates, plots of $-d[\text{NPH}]/dt$ vs. the second exponent of the initial NPH concentration $[\text{NPH}]_0^2$ (Figure S1, Supporting Information) were also linear ($R = 99.41$), reinforcing that the reaction is indeed second-order with respect to the 2-nitropropane concentration (Table 4; Experiments 1–4). This means that $m = 2$ in Equation (9).

Kinetic measurements of the reaction rate with respect to catalyst concentration (Table 4; Experiments 3, 5–9) indic-

Table 4. Kinetic data for the copper-catalysed oxygenation of 2-nitropropane in DMF solution

Expt. ^[a] no.	Temp. °C	10 ³ [O ₂] mol dm ⁻³	[Cu] mol dm ⁻³	[NPH] mol dm ⁻³	10 ⁵ k_{cat}' mol ⁻¹ dm ³ s ⁻¹	R ^[b] %	10 ² k_{cat} s ⁻¹ mol ⁻³ dm ⁹	10 ⁵ $-d[\text{NPH}]/dt$ mol dm ⁻³ s ⁻¹
1	90	8.251	0.086	0.499	4.624	99.87	6.54 ± 0.19	1.469
2	90	8.251	0.086	0.853	4.579	99.58	6.47 ± 0.31	3.330
3	90	8.251	0.086	1.077	4.629	99.38	6.55 ± 0.40	4.843
4	90	8.251	0.086	1.341	2.745	99.70	3.88 ± 0.10	6.678
5	90	8.251	0.032	1.077	1.575	99.59	5.91 ± 0.22	
6	90	8.251	0.064	1.077	2.992	99.81	5.66 ± 0.18	
7	90	8.251	0.114	1.104	6.683	99.63	7.09 ± 0.30	
8	90	8.251	0.143	1.077	6.639	99.34	5.63 ± 0.29	
9	90	8.251	0.200	1.077	9.141	99.55	5.54 ± 0.21	
10	90	1.650	0.086	1.077	0.995	99.59	7.01 ± 0.31	
11	90	4.850	0.086	1.077	3.120	99.23	7.48 ± 0.37	
12	90	7.686	0.086	1.077	4.251	98.88	6.45 ± 0.38	
13	90	9.381	0.086	1.077	5.972	98.54	7.43 ± 0.63	
14	90	11.30	0.086	1.077	7.221	98.67	7.46 ± 0.58	
							5.37 ± 0.34 ^[c]	
15	95	8.562	0.086	1.077	8.455	99.85	11.5 ± 0.35	
16	100	7.907	0.086	1.077	13.39	99.24	19.8 ± 0.72	
17	100	7.907	0.043	0.539	6.222	99.85	18.3 ± 0.53 ^[d]	
18	100	7.907	0.043	0.539	7.208	99.93	21.2 ± 0.67 ^[e]	

^[a] In 30 mL of DMF, the amount of tmeda is equimolar to copper. ^[b] Correlation coefficients of least-squares regressions. ^[c] Mean value of the kinetic constant k and its standard deviation $\sigma(k)$ were calculated as $k = (\sum w_i k_i / \sum w_i)$ and $\sigma(k) = [\sum w_i (k_i - k)^2 / (n - 1) \sum w_i]^{1/2}$, where $w_i = 1/\sigma_i^2$. ^[d] Cu^{II}(NO₂)₂(tmeda) was used as catalyst instead of Cu⁰. ^[e] Cu^{II}(NP)₂(tmeda) was used as catalyst instead of Cu⁰.

ate a first-order dependence. Plots of k_{cat}' vs. $[\text{Cu}]$ for the above experiments gave a straight line with a correlation coefficient of 99.10% (Figure S2, Supporting Information).

The experiments performed at different dioxygen concentrations (calculated from literature data assuming the validity of Dalton's law, the dissolved concentration of O_2 being $8.25 \times 10^{-3} \text{ mol dm}^{-3}$ at 90°C and 760 Torr O_2 pressure) show that the reaction is first order with respect to the dioxygen concentration (Table 4; Experiments 3, 10–14). Plotting k_{cat}' against $[\text{O}_2]$ for the above experiments resulted in a straight line with a correlation coefficient of 99.61% (Figure S3, Supporting Information). According to the kinetic data obtained the oxygenation of 2-nitropropane obeys an overall fourth-order reaction rate with $m = 2$, $n = q = 1$ in Equation (9), from which a mean value of the kinetic constant k_{cat} of $(5.37 \pm 0.34) \times 10^{-2} \text{ mol}^{-3} \text{ L}^3 \text{ s}^{-1}$ at 363.16 K was obtained (Table 4).

The catalytic oxygenation reactions of 2-nitropropane by $\text{Cu}^{\text{II}}(\text{NO}_2)_2(\text{tmeda})$ and $\text{Cu}^{\text{II}}(\text{NP})_2(\text{tmeda})$ complexes as catalysts were also carried out (Table 4; Experiments 17–18). It can be seen that the mean value of the kinetic constant for $\text{Cu}^{\text{II}}(\text{NO}_2)_2(\text{tmeda})$ and $\text{Cu}^{\text{II}}(\text{NP})_2(\text{tmeda})$ complexes are very similar to those found in the reactions, where the catalyst was prepared “in situ”, suggesting that the two complexes above were involved in the catalytic process when copper metal was used as the catalyst precursor.

The activation parameters for the catalytic oxygenation reaction were determined from the temperature dependence of the kinetic constant k_{cat} . The Arrhenius plot of $\log k_{\text{cat}}$ vs. $1/T$ (Figure S4, Supporting information) using the k_{cat} values at 363.16, 368.16 and 373.16 K (Table 4; Experiments 1–14, 15–16) was linear with a correlation coefficient of 99.27%. From the slope and the ordinate intercept of this line the parameters $E_a = 131 \pm 4 \text{ kJ mol}^{-1}$, $\Delta H^\ddagger = 127 \pm 4 \text{ kJ mol}^{-1}$ and $\Delta S^\ddagger = 80 \pm 13 \text{ J mol}^{-1} \text{ K}^{-1}$ were calculated.

In order to shed light on the kinetic scenery of the elementary steps of these catalytic reactions we also studied the kinetics of the oxygenation of the proposed interme-

diate $\text{Cu}^{\text{II}}(\text{NP})_2(\text{tmeda})$. The oxygenation of $[\text{Cu}^{\text{II}}(\text{NP})_2(\text{tmeda})]$ affords a stoichiometry corresponding to Equation (11) by the use of parallel gas-volumetric and GC measurements.



Figure 6 shows a typical concentration vs. time curve for $[\text{Cu}^{\text{II}}(\text{NP})_2(\text{tmeda})]$ obtained by the measured dioxygen uptake. The reaction between $[\text{Cu}^{\text{II}}(\text{NP})_2(\text{tmeda})]$ and dioxygen was performed in DMF solution and examined in the temperature range 303.16 to 318.16 K. Experiments were also carried out at different dioxygen concentrations. The experimental conditions are summarised in Table 5.

A simple rate law for the stoichiometric reaction between $[\text{Cu}^{\text{II}}(\text{NP})_2(\text{tmeda})]$ and dioxygen is given in Equation (12).

$$-\text{d}[\text{Cu}^{\text{II}}(\text{NP})_2(\text{tmeda})]/\text{d}t = k_s[\text{Cu}^{\text{II}}(\text{NP})_2(\text{tmeda})]^m[\text{O}_2]^n \quad (12)$$

In order to determine the rate dependence on the various reactants, oxygenation runs were performed at different $[\text{Cu}^{\text{II}}(\text{NP})_2(\text{tmeda})]$ concentrations (Table 5; Experiments 1–4), and at different dioxygen pressures (Table 5; Experiments 4–7). Assuming a constant concentration of the dioxygen during each reaction the pseudo-first-order rate law according to Equation (13) is obtained, where $k_s' = k_s[\text{O}_2]^n$.

$$-\text{d}[\text{Cu}^{\text{II}}(\text{NP})_2(\text{tmeda})]/\text{d}t = k_s'[\text{Cu}^{\text{II}}(\text{NP})_2(\text{tmeda})]^m \quad (13)$$

Plots of $\log[\text{Cu}^{\text{II}}(\text{NP})_2(\text{tmeda})]$ vs. time were linear in Experiments 1–10, indicating that the reaction is first-order with respect to the $\text{Cu}^{\text{II}}(\text{NP})_2(\text{tmeda})$ concentration. Columns k_s' and R in Table 5 report slopes and the correlation coefficients obtained by the least-squares method for these linear regressions. A typical first-order plot is shown in Figure 6 (Table 5; Experiment 4).

From variations of the reaction rates, plots of $-\text{d}[\text{Cu}^{\text{II}}(\text{NP})_2(\text{tmeda})]/\text{d}t$ (v_0) vs. $[\text{Cu}^{\text{II}}(\text{NP})_2(\text{tmeda})]$ (Figure S5, Supporting Information) were also linear ($R = 98.46$), reinforcing that the reaction is indeed first-order with respect to the $\text{Cu}^{\text{II}}(\text{NP})_2(\text{tmeda})$ concentration (Table 5; Experiments 1–4). This means that $m = 1$ in Equation (12).

Experiments carried out at different dioxygen concentrations (calculated from literature data assuming the validity of Dalton's law, the dissolved concentration of O_2 being $5.36 \times 10^{-3} \text{ mol dm}^{-3}$ at 40°C and 760 Torr O_2 pressure) show that the reaction is first-order with respect to the dioxygen concentration (Table 5; Experiments 4–7). Plotting $-\text{d}[\text{Cu}^{\text{II}}(\text{NP})_2(\text{tmeda})]/\text{d}t$ (v_0) against $[\text{O}_2]$ for the above four experiments resulted in a straight line with a correlation coefficient of 99.41% (Figure S6, Supporting Information). According to the kinetic data obtained, the oxygenation of $\text{Cu}^{\text{II}}(\text{NP})_2(\text{tmeda})$ obeys an overall second-order rate equation with $m = n = 1$ in Equation (12), from which a mean value of the kinetic constant k_s of $(0.46 \pm 0.02) \text{ mol}^{-1} \text{ dm}^3 \text{ s}^{-1}$, at 313.16 K, was obtained (Table 5).

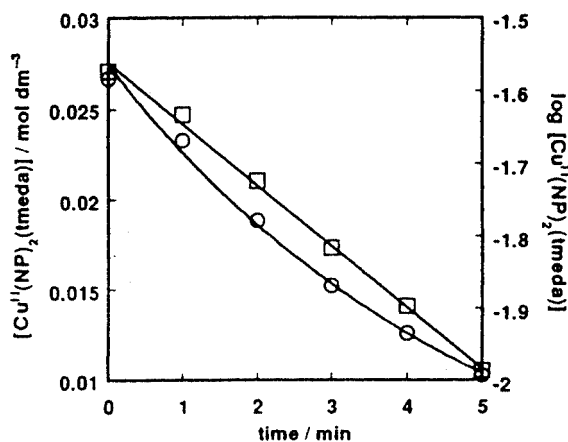


Figure 6. The time course for the oxygenation of $[\text{Cu}^{\text{II}}(\text{NP})_2(\text{tmeda})]$ (o) and plot of $\log[\text{Cu}^{\text{II}}(\text{NP})_2(\text{tmeda})]$ vs. time for the oxygenation of $[\text{Cu}^{\text{II}}(\text{NP})_2(\text{tmeda})]$ (Experiment 4, Table 5)

Table 5. Kinetic data for the stoichiometric oxygenation of $[\text{Cu}^{\text{II}}(\text{NP})_2(\text{tmeda})]$ in DMF solution

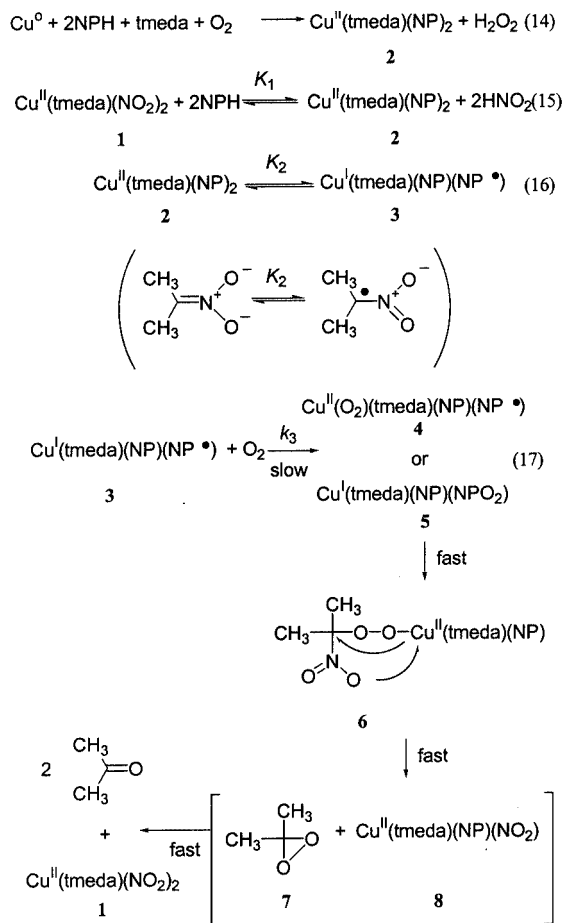
Expt. ^[a] no.	Temp. °C	$10^3[\text{O}_2]$ mol dm^{-3}	$10^2[\text{Cu}]^{\text{[a]}}$ mol dm^{-3}	$10^3k_s'$ s^{-1}	$R^{\text{[b]}}$ %	k_s $\text{s}^{-1} \text{mol}^{-1} \text{dm}^3$	$10^5 - \text{d}[\text{Cu}]/\text{dt}$ $\text{mol dm}^{-3} \text{s}^{-1}$
1	40	5.36	0.67	2.835 ± 0.166	99.37	0.529 ± 0.031	1.901 ± 0.11
2	40	5.36	1.33	2.604 ± 0.107	99.70	0.486 ± 0.020	3.473 ± 0.14
3	40	5.36	2.00	2.422 ± 0.123	99.45	0.452 ± 0.023	4.846 ± 0.25
4	40	5.36	2.67	2.256 ± 0.107	99.67	0.421 ± 0.020	6.015 ± 0.28
5	40	1.07	2.67	0.623 ± 0.022	99.55	0.583 ± 0.021	1.663 ± 0.06
6	40	2.68	2.67	1.283 ± 0.067	98.44	0.479 ± 0.025	3.416 ± 0.18
7	40	3.75	2.67	0.533 ± 0.041	99.85	0.409 ± 0.011 $0.456 \pm 0.024^{\text{[c]}}$	4.090 ± 0.11
8	30	4.84	2.67	1.050 ± 0.038	98.34	0.217 ± 0.008	2.720 ± 0.10
9	35	5.10	2.67	1.683 ± 0.076	99.60	0.330 ± 0.015	4.649 ± 0.21
10	45	5.52	2.67	2.743 ± 0.049	99.94	0.497 ± 0.009	7.314 ± 0.13

^[a] In 30 mL of DMF. ^[b] Correlation coefficients of least-squares regressions. ^[c] Mean value of the kinetic constant k and its standard deviation $\sigma(k)$ were calculated as $k = (\sum w_i k_i / \sum w_i)$ and $\sigma(k) = [\sum w_i (k_i - k)^2 / (n - 1) \sum w_i]^{1/2}$, where $w_i = 1/\sigma_i^2$.

The activation parameters for the stoichiometric oxygenation reaction were determined from the temperature dependence of the kinetic constant k_s . The Arrhenius plot of $\log k_s$ vs. $1/T$ (Figure S7, Supporting Information) using the k_s values at 303.16, 308.16, 313.16 and 318.16 K (Table 5; Experiments 4, 8–10) was linear with a correlation coefficient of 99.48%. From the slope and the ordinate intercept of this line the parameters $E_a = 38 \pm 1 \text{ kJ mol}^{-1}$, $\Delta H^\ddagger = 35 \pm 1 \text{ kJ mol}^{-1}$ and $\Delta S^\ddagger = -142 \pm 13 \text{ J mol}^{-1} \text{ K}^{-1}$ were calculated. Values of the activation parameters indicate that the oxidation of $\text{Cu}^{\text{II}}(\text{NP})_2(\text{tmeda})$ is a bimolecular reaction involving the associative transition state of $\text{Cu}^{\text{II}}(\text{NP})_2(\text{tmeda})$ and molecular oxygen; k_{cat} is substantially smaller than k_s since in the former the pre-equilibrium constants K_1 and K_2 are also involved, and K_1 and K_2 are small. The equilibria according to Equations (15) and (16) are shifted to the left side. A comparison of the activation enthalpies and entropies of the catalytic and stoichiometric reactions clearly shows that the stoichiometric reaction is enthalpy-driven while in the case of the catalytic reaction the positive ΔS^\ddagger and the larger ΔH^\ddagger values show a different situation. Here the contribution of the entropy seems to be more and the enthalpy less dominant. This may be explained by the effect of the pre-equilibrium according to Equation (15), since K_1 is involved in k_{cat} thus causing this difference.

Based on the kinetic data on the copper-catalysed oxygenation of 2-nitropropane to acetone, a probable mechanism is proposed as shown in Scheme 1. According to that, the first step is the formation of the complex $\text{Cu}^{\text{II}}(\text{tmeda})(\text{NP})_2$ (**2**) from copper powder, 2-nitropropane, tmeda, and dioxygen [Equation (14)] or from $\text{Cu}^{\text{II}}(\text{tmeda})(\text{NO}_2)_2$ through substitution of NO_2^- by NP^- in a pre-equilibrium in the catalytic cycle [Equation (15)]. This is then followed by an intramolecular electron transfer [Equation (16)] from the ligand 2-nitropropanate to the copper(II) ion resulting in a (2-nitropropyl radical)copper(I) complex $\text{Cu}^{\text{I}}(\text{tmeda})(\text{NP})(\text{NP}^\bullet)$ (**3**). This equilibrium is largely shifted to the left (K_2 is rather small). All attempts to detect the

radical by EPR spectroscopy failed. The 2-nitropropanate anion does not react with $^3\text{O}_2$.^[34] The absence of the electron transfer from $\text{Cu}^{\text{II}}(\text{tmeda})(\text{NP})_2$ to dioxygen could also be proved by the test for free O_2^- with nitroblue tetrazolium (NBT), where no reduction of the added dye to the blue formazan took place excluding the formation of free O_2^- .^[35]

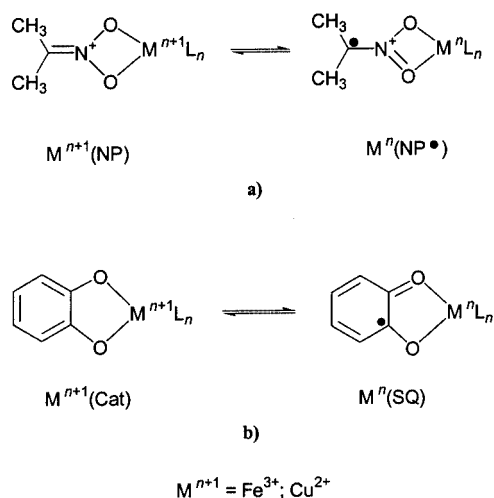


Scheme 1

In the complex $\text{Cu}^{\text{I}}(\text{tmeda})(\text{NP})(\text{NP}^{\bullet})$ (**3**) there are two redox-active centres, namely the nitropropanyl radical NP^{\bullet} and the copper(I) ion.

The biradical dioxygen may react at both redox-active sites of the complex $\text{Cu}^{\text{I}}(\text{tmeda})(\text{NP})(\text{NP}^{\bullet})$, in a radical-radical reaction with the coordinated radical ligand NP^{\bullet} leading to the peroxo intermediate **5**, or in an oxidative addition of O_2 to the copper(I) ion giving the (superoxo)copper(II) complex **4**, as found in the case of many other copper(I) complexes.^[36] Both mechanistic assumptions satisfy the kinetic data, but we believe that the reaction of the copper(I) centre of **3** with O_2 is more probable. We have observed earlier that radical ligands bound to metal ions that cannot be oxidised (e.g. Cu^{II} , Fe^{III} , etc)^[37] do not react with O_2 at all, or undergo very slow reactions only. The (superoxo)copper(II) complex **4** then undergoes an intramolecular radical-radical reaction of the coordinated ligands O_2^- and NP^{\bullet} resulting in the peroxide species **6**. This then decomposes to the mixed-ligand copper(II) complex **8** and 1,1-dimethyldioxirane (**7**). The 1,1-dimethyldioxirane (**7**) then oxygenates the coordinated NP^- in **8** resulting in $\text{Cu}^{\text{II}}(\text{tmeda})(\text{NO}_2)_2$ and acetone. The 2-nitropropane once again replaces the nitrito ligand in **1** and so closes the catalytic cycle. Previous studies have shown, that dimethyldioxirane oxidation of nitronate anions affords the corresponding carbonyl product.^[38]

As a conclusion it can be said, that the present work provides further support to the key role of redox-active ions in these oxygenation reactions, which may be regarded as functional models for 2-nitropropane dioxygenase. We believe that there is a valence tautomerism between $\text{Cu}^{\text{II}}(\text{NP})$ and $\text{Cu}^{\text{I}}(\text{NP}^{\bullet})$ due to intramolecular electron transfer from the ligand to the metal ion (Scheme 2a). In this sense of the activation process the ligand is transformed to a radical and copper(II) to copper(I). The latter then reacts with dioxygen to form a peroxidic species, which transforms to the (nitrito)copper(II) complex and acetone. At the intradiol cleavage of catechols either by iron-^[39] or copper-containing^[40] catechol 1,2-dioxygenases along with model studies^[41] it has



Scheme 2

been proven that valence isomerism plays an important role (Scheme 2b). The molecular orbitals involved in this process are close to each other in energy and so the electron transfer is easily feasible. The equilibrium depends of course on auxiliary ligands as shown in the case of copper catecholate complexes, whereas soft ligands prefer the lower oxidation state of the metal ion.^[42] A similar behaviour with (nitropropane)iron complexes is also to be expected as a key step in these oxygenations. Further work is in progress on the design and elucidation of iron-containing functional 2-nitropropane dioxygenase models.

Experimental Section

Materials and Methods: Analytical-grade reagents were used throughout. Copper powder (Aldrich), 2-nitropropane (Fluka), *N,N,N',N'*-tetramethylethylenediamine (Aldrich), 2,2'-bipyridine (Aldrich), and 1,10-phenanthroline (Aldrich) were used as supplied. DMF (Aldrich) was purified by azeotropic distillation with benzene and water and stored under argon.^[43] Gaseous dioxygen from Messer Griesheim was 99.6% and passed through P_2O_5 and Blaugel in order to remove traces of water and other impurities. IR spectra were recorded with a Specord IR-75 (Carl Zeiss) spectrometer on either Nujol or KBr pellets. Electronic spectra were measured with a Shimadzu UV-160A spectrophotometer using quartz cells. GC analyses were performed with HP 5830A and HP 5890 gas chromatographs equipped with a flame ionisation detector and CP SIL 8CB column. GC-MS measurements were recorded with an HP 5890II/5971 GC/MSD instrument at 75 eV.

Stoichiometric Oxygenation: In a typical stoichiometric reaction 2-nitropropane (0.36 mL, 3 mmol), copper metal (0.10 mg, 1.5 mmol) and tmeda (0.225 mL, 1.5 mmol) in DMF (30 mL) were stirred at 90 °C under dioxygen for 60 min. The stoichiometry of the reactions was investigated by gas volumetric (O_2), spectrophotometric (NO_2),^[44] titrimetric (NO_3)^[45] and GC measurements (acetone), and the presence of H_2O_2 was determined by iodometry^[46] (Table 1.). Then diethyl ether was layered on the solution and left at −20 °C for 2 h to afford a green solid, which was filtered off and recrystallised from acetonitrile to give $[\text{Cu}(\text{tmeda})(\text{NO}_3)(\text{NO}_2)]$ as green crystals (0.11 g, 25%). M.p. 172 °C (dec.). $\text{C}_6\text{H}_{16}\text{CuN}_4\text{O}_5$ (287.7): calcd. C, 25.03, H 5.60, Cu 22.07, N 19.46; found C 25.4, H 5.49, Cu 22.43, N 19.31. UV/Vis (DMF): λ_{max} ($\log \epsilon/\text{mol}^{-1} \text{ dm}^3 \text{ cm}^{-1}$) = 276 (3.66), 365 (3.16), 642 nm (2.300). IR (KBr): $\tilde{\nu}_{\text{max}}$ = 2976 m, 2938 w, 2888 w, 1567 m, 1470 vs, 1387 s, 1361 vs, 1284 m, 1161 vs, 1046 s, 1020 s, 1001 m, 956 s, 846 m, 814 s, 769 cm^{-1} m. μ_{eff} = 2.07 BM. The ratio $\text{NO}_3^-/\text{NO}_2^-$ in the complex was 1:1.2.

Preparation of $[\text{Cu}^{\text{II}}(\text{NP})_2(\text{tmeda})]$: $[\text{Cu}(\text{OMe})_2]$ (3.14 g, 25 mmol) was dissolved in MeOH (20 mL); tmeda (3.78 mL, 25 mmol) and 2-nitropropane (4.5 mL, 50 mmol) were added and the mixture was stirred under argon at room temperature for 20 h. The solvent was then removed in vacuo and the remaining oily residue was treated with diethyl ether, filtered off and dried to give a green powder (7.60 g, 85%). M.p. 95 °C (dec.). $\text{C}_{12}\text{H}_{28}\text{CuN}_4\text{O}_4$ (355.9): calcd. C 39.88, H 7.45, N 15.49; found C 40.50, H 7.93, N 15.74. IR (KBr): $\tilde{\nu}$ = 2925 w, 1612 vs, 1464 vs, 1393 w, 1291 w, 1162 vs, 1123 vs, 1059 m, 1033 m, 956 m, 943 s, 814 s, 782 m, 634 m, 402 cm^{-1} m. UV/Vis (DMF): λ_{max} ($\epsilon/\text{L mol}^{-1} \text{ cm}^{-1}$) = 314 (978.5), 727 nm (76.7). μ_{eff} = 1.92 BM. On recrystallisation from THF green single

crystals of $[\text{Cu}^{\text{II}}(\text{NP})_2(\text{tmeda})]$ were formed suitable for X-ray diffraction.

Kinetic Experiments: Kinetic measurement were carried out at atmospheric pressure, at constant partial pressure of dioxygen with vigorous stirring in a thermostatted reaction vessel equipped with a syringe inlet for taking samples at regular time intervals. The samples taken were chilled, stored at dry-ice temperature and then submitted for GC or GC-MS analysis. Dioxygen uptakes were also measured in a constant-pressure gas-volumetric apparatus. The volume of absorbed dioxygen was read periodically using a gas burette. The amount of nitrous acid was determined spectrophotometrically^[44] after diazotization of sulfanylic acid and successive coupling with 1-aminonaphthalene, and was found in each case to be nearly equal to that of acetone. The catalytic reactions were carried out by preparing the catalyst from copper metal, tmeda, and 2-nitropropane in DMF under dioxygen. After about 10–15 min, the mixture gave a green homogeneous solution by dissolving the copper metal. Thereafter, the reaction was monitored by analysing the amount of products (acetone and acetone oxime) and the starting 2-nitropropane by GLC. In a typical oxygenation of 2-nitropropane to acetone and acetone oxime, the copper metal (191 mg, 3 mmol), 2-nitropropane (3.6 mL, 40 mmol), tmeda (0.45 mL, 3 mmol) and DMF (30 mL) were stirred under dioxygen at 95 °C. After dissolution of the copper powder (10 min), samples were taken at ca. 10-min intervals, cooled to dry-ice temperature and then subjected to GLC analysis. The solubility of dioxygen in DMF at 95 °C was taken as $8.56 \times 10^{-3} \text{ M}$.^[47] The validity of Dalton's law was assumed for the calculation of dioxygen concentration at different partial pressures.^[48] Diethyl ether was layered on the solution and left at –20 °C for 2 h to afford a green solid, which was filtered off and recrystallised from ethanol to give $[\text{Cu}^{\text{II}}(\text{tmeda})(\text{NO}_2)_2]$ as green crystals. M.p. 197 °C (dec.). $\text{C}_6\text{H}_{16}\text{CuN}_4\text{O}_4$ (271.7): calcd. C 26.51, H 5.93, N 20.62; found C 25.7, H 5.72, N 19.91. UV/Vis (DMF): λ_{max} ($\log \varepsilon/\text{mol}^{-1} \text{ dm}^3 \text{ cm}^{-1}$) = 271 (3.66), 222 (3.43) and 648 nm (2.17). IR (KBr): $\tilde{\nu}_{\text{max}}$ = 2983 m, 2941 m, 2899 m, 1477 s, 1468 s, 1360 vs, 1286 m, 1249 m, 1165 vs, 1101 m, 1041 m, 1021 m, 1000 m, 953 s, 845 m, 808 s, 770 m, 593 cm^{-1} m. The stoichiometric oxygenation of $[\text{Cu}^{\text{II}}(\text{NP})_2(\text{tmeda})]$ was carried out in a thermostatted constant-pressure gas-volumetric apparatus. The volume of absorbed dioxygen was read periodically using a gas burette.

X-ray Crystallography: Crystallographic and experimental details of the data collection and refinement of the structures of $\text{Cu}^{\text{II}}(\text{NO}_2)_2(\text{tmeda})$ and $\text{Cu}^{\text{II}}(\text{NP})_2(\text{tmeda})$ are reported in Table 6, while the molecular structures are depicted in Figures 4 and 5. The intensity data of $\text{Cu}^{\text{II}}(\text{NO}_2)_2(\text{tmeda})$ were collected with a KappaCCD single-crystal diffractometer, using the graphite-monochromated Mo- K_α radiation and ϕ -scan technique. The structure was solved by direct and difmap methods (SIR92),^[49] and refined on F^2 using full-matrix least-squares methods (Maxus).^[50] The intensity data of $\text{Cu}^{\text{II}}(\text{NP})_2(\text{tmeda})$ were collected with an Enraf–Nonius CAD-4 single-crystal diffractometer, using graphite-monochromated Mo- K_α radiation and $\omega/2\theta$ -scan technique. The structure was solved by direct and difmap methods (SHELXS-97),^[51] and refined with full-matrix least-squares refinement on F^2 (SHELXL-97).^[52] CCDC-167599 (1) and -167598 (2) contain the supplementary crystallographic data for this paper. These data can be obtained free of charge at www.ccdc.cam.ac.uk/conts/retrieving.html or from the Cambridge Crystallographic Data Centre, 12, Union Road, Cambridge CB2 1EZ, UK [Fax: (internat.) + 44-1223/336-0333; E-mail: deposit@ccdc.cam.ac.uk].

Table 6. Crystal data, data collection parameters and structure refinement of compounds $\text{Cu}^{\text{II}}(\text{NO}_2)_2(\text{tmeda})$ (1) and $\text{Cu}^{\text{II}}(\text{NP})_2(\text{tmeda})$ (2)

	1	2
Empirical formula	$\text{C}_6\text{H}_{16}\text{CuN}_4\text{O}_4$	$\text{C}_{12}\text{H}_{31}\text{CuN}_4\text{O}_6$
Crystal system	monoclinic	tetragonal
Space group	$P21/n$	$P421c$
Z	4	4
Temperature [K]	293(2)	293(2)
$d_{\text{calcd.}}$ [g/cm^3]	1.555	1.314
a [Å]	7.5758(2)	11.862(1)
b [Å]	12.5094(7)	11.862(1)
c [Å]	12.5291(6)	14.047(1)
α [°]	90	90
β [°]	102.091(3)	90
γ [°]	90	90
V [Å ³]	1161.0(1)	1976.5(3)
μ [mm^{-1}]	1.88	1.135
$F(000)$	564	832
Index ranges	$0 \leq h \leq 8$ $0 \leq k \leq 15$ $-15 \leq l \leq 15$	$-19 \leq h \leq 19$ $-19 \leq k \leq 19$ $-22 \leq l \leq 22$
Data collected	2263	9518
Reflections [$I > 3\sigma(I)$]	1894	2134
Parameters	136	109
$R = \Sigma F_o - F_c /\Sigma F_o $	0.032	0.0323
$wR = [w(F_o^2 - F_c^2)^2/w(F_c^2)^2]^{1/2}$	0.045	0.0682
GOF	1.537	0.814

Supporting Information: Kinetic diagrams for stoichiometric and catalytic oxygenations are available (see also footnote on the first page of this article).

Acknowledgments

Financial support of the Hungarian National Research Fund (OTKA T-30400) and Ministry of Education (FKFP-0446/1999) is gratefully acknowledged.

[1] H. W. Pinnick, *Org. React.* **1990**, 38, 655.

[2] [2a] J. E. McMurry, J. Melton, *Canad. J. Org. Chem.* **1973**, 38, 4367. [2b] J. E. McMurry, *Acc. Chem. Res.* **1974**, 7, 281. [2c] R. Kirchoff, *Tetrahedron Lett.* **1976**, 17, 2533.

[3] P. S. Vankar, R. Rathore, S. Chandrasekaran, *Synth. Commun.* **1987**, 17, 195.

[4] F. Urpi, J. Vilarrasa, *Tetrahedron Lett.* **1990**, 31, 7499.

[5] E. Keinan, Y. Mazur, *J. Am. Chem. Soc.* **1977**, 99, 3861.

[6] G. A. Olah, M. Arvanahi, Y. D. Vankar, G. K. S. Prakash, *Synthesis* **1980**, 662.

[7] [7a] H. Schechter, F. T. Williams, *J. Org. Chem.* **1962**, 27, 3699.

[7b] F. Freeman, A. Yeramy, *J. Org. Chem.* **1970**, 35, 2061. [7c] F. Freeman, D. K. Lin, *J. Org. Chem.* **1971**, 36, 1335. [7d] N. Kornblum, A. S. Erickson, W. J. Kelly, B. Henggeler, *J. Org. Chem.* **1982**, 47, 4534. [7e] K. Steliou, M. A. Poupart, *J. Org. Chem.* **1985**, 50, 4971.

[8] G. A. Olah, B. G. B. Gupta, *Synthesis* **1980**, 44.

[9] M. R. Galobardes, H. W. Pinnick, *Tetrahedron Lett.* **1981**, 22, 5235.

[10] J. E. McMurry, J. Melton, H. Padgett, *J. Org. Chem.* **1974**, 39, 259.

[11] J. R. Williams, L. R. Ungler, R. H. Moore, *J. Org. Chem.* **1978**, 43, 1271.

- [12] P. A. Bartlett, F. R. Green, T. R. Webb, *Tetrahedron Lett.* **1977**, 18, 331.
- [13] D. J. T. Porter, H. J. Bright, *J. Biol. Chem.* **1977**, 252, 4361.
- [14] D. J. T. Porter, J. G. Voet, H. J. Bright, *J. Biol. Chem.* **1973**, 248, 4400.
- [15] T. W. Chan, T. C. Bruice, *Biochemistry* **1978**, 17, 4784.
- [16] I. Yokoe, T. C. Bruice, *J. Am. Chem. Soc.* **1975**, 97, 450.
- [17] T. C. Bruice, *Adv. Chem. Ser.* **1980**, 191, 89.
- [18] [18a] H. N. Little, *J. Biol. Chem.* **1951**, 193, 347. [18b] H. N. Little, *J. Biol. Chem.* **1957**, 229, 231.
- [19] J. A. E. Molina, M. Alexander, *J. Bacteriol.* **1971**, 105, 489.
- [20] T. Kido, T. Yamamoto, K. Soda, *Arch. Microbiol.* **1975**, 106, 165.
- [21] T. Kido, T. Yamamoto, K. Soda, *J. Bacteriol.* **1976**, 126, 1261.
- [22] T. Kido, K. Soda, T. Suzuki, K. Asada, *J. Biol. Chem.* **1976**, 251, 6994.
- [23] É. Balogh-Hergovich, G. Speier, G. Huttner, L. Zsolnai, *Inorg. Chem.* **1998**, 37, 6535.
- [24] É. Balogh-Hergovich, J. Kaizer, G. Speier, *Chem. Lett.* **1996**, 573.
- [25] [25a] R. T. Stibrany, J. A. Potenza, H. S. Shugar, *Inorg. Chim. Acta* **1996**, 33, 243. [25b] R. A. Leising, S. A. Kubow, L. F. Szeptura, T. J. Takeuchi, *Inorg. Chim. Acta* **1996**, 167, 245. [25c] M. A. Andrew, T. C-T Chang, C-W. F. Cheng, L. V. Kapustay, K. P. Kelly, M. J. Zweifel, *Organometallics* **1984**, 3, 1479. [25d] M. Green, T. A. Kuc, S. H. Taylor, *J. Chem. Soc.* **1971**, 2334. C. A. Bignozzi, C. Chiorboli, Z. Murtaza, V. E. Jones, T. J. Meyer, *Inorg. Chem.* **1993**, 32, 1036.
- [26] A. Santoro, A. D. Mighell, C. W. Reimann, *Acta Crystallogr., Sect. B* **1970**, 26, 979.
- [27] F. S. Stephens, *J. Chem. Soc. A* **1969**, 2081.
- [28] M. Gargano, N. Ravasio, M. Rossi, A. Tiripicchio, C. M. Tiripicchio, *J. Chem. Soc., Dalton Trans.* **1989**, 921.
- [29] S. Youngme, S. Tonpho, K. Chinnakali, S. Chantrapromma, H. Fun, *Polyhedron* **1999**, 18, 851.
- [30] A. J. Blake, S. J. Hill, P. Hubberstey, *Chem. Commun.* **1998**, 1587.
- [31] L. Pauling, *The Nature of the Chemical Bond*, 3rd ed., Cornell University Press, Ithaca, New York, **1960**.
- [32] T. Kovács, G. Speier, M. Réglér, M. Giorgi, A. Vértés, G. Vankó, *Chem. Commun.* **2000**, 469.
- [33] O. Simonsen, *Acta Crystallogr., Sect. B* **1973**, 29, 2600.
- [34] J. R. Williams, L. R. Unger, R. H. J. Moore, *J. Org. Chem.* **1978**, 43, 1271.
- [35] B. H. J. Bielski, H. W. Richter, *J. Am. Chem. Soc.* **1977**, 99, 3019.
- [36] K. D. Karlin, S. Kaderli, A. D. Zuberbühler, *Acc. Chem. Res.* **1997**, 30, 139.
- [37] G. Speier, B. Tapodi, unpublished results.
- [38] W. Adam, M. Makosza, C. R. Saha-Moller, C. G. Zhao, *Synlett* **1998**, 12, 1335.
- [39] L. Que, Jr., R. Y. N. Ho, *Chem. Rev.* **1996**, 96, 2607.
- [40] G. Speier, *New J. Chem.* **1994**, 18, 143.
- [41] G. Speier, Z. Tyeklár, L. Szabó, P. Tóth, C. G. Pierpont, D. N. Hendricson, "Evidence for Substrate Activation of Copper Catalyzed Intradiol Cleavage in Catechols", in *The Activation of Dioxygen and Homogeneous Catalytic Oxidation* (Eds.: D. H. R. Barton, A. E. Martell, D. T. Sawyer), Plenum Press, New York, **1993**, pp. 423–436.
- [42] J. Rall, M. Wanner, M. Albrecht, F. M. Hornung, W. Kaim, *Chem. Eur. J.* **2000**, 5, 2802.
- [43] D. D. Perrin, W. L. Armarego, D. R. Perrin, *Purification of Laboratory Chemicals*, 2nd ed., Pergamon, New York, **1990**.
- [44] E. Sawicki, *Talanta* **1963**, 10, 641.
- [45] A. Steyermark, *Quantitative Organic Microanalysis*, 2nd ed., Academic Press, New York, **1961**, p. 188.
- [46] A. I. Vogel, *A Text Book of Quantitative Inorganic Analysis*, 3rd ed., Wiley, New York, **1961**, p. 343.
- [47] A. Kruis, *Landolt-Börnstein*, Springer, Berlin, **1976**, vol. 4, part 4, p. 269.
- [48] G. Ram, A. R. Sharaf, *J. Ind. Chem. Soc.* **1968**, 45, 13.
- [49] S. Mackay, C. J. Gilmore, C. Edwards, N. Stewart, K. Shankland, *Maxus Computer Program for the Solution and Refinement of Crystal Structures*, Nonius (The Netherlands), MacScience (Japan), The University of Glasgow (UK), **1999**.
- [50] SIR92: A. Altomare, G. Cascarano, C. Giacovazzo, A. Guagliardi, M. C. Burla, G. Polidori, M. Camalli, *J. Appl. Crystallogr.* **1994**, 27, 435.
- [51] G. M. Sheldrick, *SHELXS-97, Program for crystal structure refinement*, Universität Göttingen, Germany, **1997**.
- [52] G. M. Sheldrick, *SHELXL-97, Program for crystal structure refinement*, Universität Göttingen, Germany, **1997**.

Received October 10, 2001

[101401]